Inorganic Chemistry

Article

pubs.acs.org/IC

# Lithium-Stuffed Diamond Polytype Zn−Tt Structures (Tt = Sn, Ge): The Two Lithium−Zinc−Tetrelides $Li_3Zn_2Sn_4$ and $Li_2ZnGe_3$

Saskia Stegmaier and Thomas. F. Fässler*

Department Chemie, Technische Universität München, Lichtenbergstraße 4, 85747 Garching, Germany

Supporting Information

**ABSTRACT:** In view of the search for alternative structures for Li ion battery materials and electron-poor framework semiconductors for thermoelectric applications, the systems Li−Zn−Tt with Tt = Ge or Sn were investigated. $Li_3Zn_2Sn_4$ and $Li_2ZnGe_3$ were obtained by high-temperature syntheses from the elements. The crystal structures of both phases were determined with single-crystal X-ray diffraction methods and the electronic structure of $Li_3Zn_2Sn_4$ was analyzed by means of DFT calculations (TB-LMTO-ASA). Both phases show diamond polytype analogous Zn−Tt networks with tetrahedrally four-coordinated Zn and Tt atoms. The new phase $Li_3Zn_2Sn_4$ crystallizes in space group $P6_3/mmc$ (No. 194) with lattice parameters $a$ = 4.528(1) Å and $c$ = 22.119(2) Å. Zn and Sn atoms are fully ordered on three sites that constitute a 6H diamond polytype like network. $Li_2ZnGe_3$ is also described in space group $P6_3/mmc$ (No. 194) with lattice parameters $a$ = 4.167(1) Å and $c$ = 6.754(1) Å. The Zn−Ge substructure is a hexagonal diamond (2H polytype) like network. The existence of such a Ge-rich Li−Zn−Ge phase has already been reported, but a full structure determination has not yet been published. No indication for an ordering of Zn and Ge atoms on different sites could be deduced from the X-ray diffraction data. Band structure calculations for $Li_3Zn_2Sn_4$ indicate that the phase is metallic, with the Fermi level at the flank of a pseudogap in the density of states curve. The topological analysis of the electron localization function (ELF) shows covalent Sn−Sn bonding and lone pair like valence basins for the Sn atoms. Concerning the appearance of the lone pair like ELF basins, a strong influence of the basis set for Li that is employed in the calculations is found.

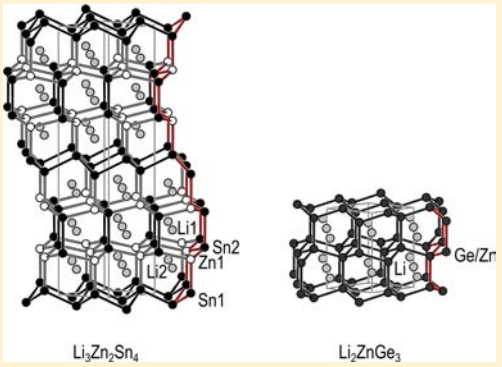


## INTRODUCTION

Networks of four-bonded atoms play a decisive role in the structural chemistry of the group 14 elements C, Si, Ge, and Sn. The archetypal diamond structure features a perfect tetrahedral coordination environment for all atoms, suited for covalently bonded networks with four valence electrons per atom and $sp^3$ hybrid orbitals. Stuffed diamond polytype like structures with Li atoms in the voids of the four-connected network are found for a number of ternary tetrelides. They can commonly be described as Zintl compounds or related polar intermetallic phases with Li as electron donor to a polyanionic network comprising group 14 (Tt) together with group 13 (Tr) or late d block metal (T) atoms. Note that the cubic stuffed diamond like structures are structurally analogous to the (half-)Heusler phases, which are studied intensively with respect to their physical properties, including potential applications in the field of thermoelectrics.[1] Furthermore, the systems reported herein also show an interesting relation to thermoelectric materials with sp-bonded framework structures as observed in the system Zn−Sb,[2−5] with special emphasis on electron-poor framework semiconductors.[6] Given recent findings on other T−Tt networks of four-connected atoms in the Na−Zn−Sn system[7,8] and in view of the search for alternative structures for Li ion battery materials,[9,10] we investigated the Li−Zn−Tt systems with Tt = Ge or Sn.

Li−Zn−Ge phases that have been structurally characterized include LiZnGe[11−13] (first described as "$Li_{1.25}ZnGe$"[14,15]), $\alpha$-$Li_2ZnGe$,[13,14,16,17] and $\beta$-$Li_2ZnGe$,[18] Li-rich $Li_8Zn_2Ge_3$,[13] and $Li_{17-\varepsilon}Zn_\varepsilon Ge_4$[19] (a Zn-doped derivative of $Li_{17}Ge_4$). $\alpha$-$Li_2ZnGe$ can be described as an electron-precise Zintl phase, which features a cubic zinc blende like Zn−Ge network stuffed with Li,[13] that is, a structure closely related to the pristine NaTl structure type. Two other phases have been identified in the system, but their structures have not been (fully) determined.[14,20] In the Li−Zn−Sn system, the phase $Li_2ZnSn$,[16,21] which also adopts a NaTl type related structure, is known. With the heavier alkali metals, only a few A−Zn−Ge phases (A = alkali metal) have been reported, including $Na_2ZnGe$, which adopts a ($Na_2CuAs$ type) structure that is completely different from that of $Li_2ZnGe$, featuring {Zn−Ge} zigzag chains with linearly coordinated Zn atoms.[22] Further, there exist the type-I clathrate $K_8Zn_4Ge_{42}$[23] with a three-dimensional network of tetrahedrally connected Zn and Ge atoms as well as $Cs_6ZnGe_8$, which shows a cluster built of two {$Ge_4$} tetrahedral units linked by a Zn atom.[24] With the exception of the Na−Zn−Sn system, which has been studied recently,[7] little is known about the A−Zn−Sn systems with the other alkali metals. With A =

Received: May 25, 2012
Published: September 4, 2012

   dx.doi.org/10.1021/ic3011037 | Inorg. Chem. 2013, 52, 2809−2816

Rb and Cs, the formally charge-balanced clathrates $A_8Zn_4Sn_{42}$ have been investigated.[25,26] The manifold Na−Zn−Sn phases show a rich diversity of polyanionic Zn−Sn substructures, including networks of interconnected icosahedral Zn−Sn clusters combined with other structure motifs (clusters or others),[27,28] isolated {Sn−Zn−Sn} units,[29] and also a network of four-bonded Zn and Sn atoms.[8] The latter is found for the Sn-rich phase $Na_5Zn_{2.28}Sn_{9.72}$.[8]

The (re)investigation of the Li−Zn−Sn system led to the new phase $Li_3Zn_2Sn_4$ with a Zn−Sn substructure of four-connected Zn and Sn atoms that can be described as an ordered coloring variant of the 6H diamond polytype structure. In the Li−Zn−Ge system, a phase with a hexagonal (2H) diamond like Zn−Ge structure part was obtained. The existence of such a phase has been reported before,[14] but a full structure determination (including atomic coordinates) has not yet been published (see above). The phase is described here as $Li_2ZnGe_3$. No indication for an ordering of Zn and Ge could be deduced from the single-crystal X-ray diffraction data for this phase.

## EXPERIMENTAL SECTION

**Synthesis.** For the syntheses of the title phases, all materials were handled in argon atmosphere using an argon-filled glovebox and other standard inert gas techniques. Zn granules (Merck), Ge pieces (99.999%, ChemPur), and Sn granules (99.999%, ChemPur) were used as received; Li was distilled before use.

$Li_3Zn_2Sn_4$ and $Li_2ZnGe_3$ were obtained from direct reactions of the elements in ratio Li/Zn/Tt = 2:1:5, employing 0.021 g of Li, 0.096 g of Zn, and 0.883 g of Sn or 0.032 g of Li, 0.148 g of Zn, and 0.821 g of Ge, respectively. In argon atmosphere, the elements were sealed in tantalum ampules, and these were placed in silica tubes, which were evacuated, sealed, and inserted in vertical resistance tube furnaces. The sample with Li, Zn, and Ge was heated to 500 °C at a rate of 2 K $min^{-1}$, held at that temperature for 5 days, and then quenched to room temperature by taking the tube out of the oven. The sample with Li, Zn, and Sn was heated to 700 °C, cooled to 50 °C, and heated to 300 °C with heating/cooling rates of 1 K $min^{-1}$. At 300 °C, it was tempered, and then it was quenched by taking the tube out of the furnace and dropping the ampule into liquid nitrogen. For the reaction with Li, Zn, and Sn, the powder XRD analysis of the product showed the reflections of $Li_3Zn_2Sn_4$ and $\beta$-Sn. The powder pattern of the product of the reaction with Li, Zn, and Ge showed the presence of $Li_2ZnGe_3$, $\alpha$-Ge, LiGe,[30] and some unindexed reflections. The single crystal used for the structure determination of $Li_3Zn_2Sn_4$ was obtained from the product of the reaction described above. For $Li_2ZnGe_3$, the single crystal for the XRD measurement was taken from a sample that was obtained from a reaction of stoichiometric amounts of the elements (Li/Zn/Ge = 2:1:3) using a temperature program similar to that for the reaction with Li, Zn, and Sn described above with an isothermal dwelling step at 300 °C. Powder XRD analysis for this sample showed $Li_2ZnGe_3$ as the main phase, $\alpha$-Ge, and some unindexed reflections.

**Powder X-ray Diffraction.** For powder XRD analysis, samples of the reaction products were finely ground, diluted with diamond powder, and sealed in glass capillaries in an argon-filled glovebox. Powder XRD data were collected with a STOE STADI P powder diffractometer equipped with an imaging plate and a linear position sensitive detector (IP-PSD and L-PSD) using Cu K$\alpha_1$ radiation ($\lambda$ = 1.54060 Å, curved Ge(111) monochromator). The STOE WIN-XPOW program package[31] was used for phase analysis.

**Single-Crystal X-ray Diffraction and Crystal Structure Determination.** Single crystals of $Li_3Zn_2Sn_4$ and $Li_2ZnGe_3$ were selected in an argon-filled glovebox equipped with a microscope. A dark silver lustrous crystal of $Li_3Zn_2Sn_4$ was mounted on a glass fiber that was subsequently fixed and sealed in a glass capillary, and single-crystal XRD data were collected at 293 K with a STOE IPDS 2T imaging plate diffractometer using Mo K$\alpha$ radiation ($\lambda$ = 0.71073 Å, graphite monochromator, rotating anode source). A total of 540 frames were collected in three $\omega$ scans ($\omega$ = 0° to 180° with $\varphi$ = 0°, 70°, and 110°), with a detector distance of 100 mm, an exposure time of 1 min, and an $\omega$ increment of 1° per frame. The STOE X-AREA software[32] was used for data processing. A numerical absorption correction was applied with X-RED[33]/X-SHAPE.[34] A dark silver lustrous crystal of $Li_2ZnGe_3$ was mounted on a glass fiber, and single-crystal XRD data were collected at 125 K (Oxford Instruments Cryojet cooling system, nitrogen jet) with an Oxford Xcalibur3 diffractometer with a Sapphire 3 CCD detector using Mo K$\alpha$ radiation ($\lambda$ = 0.71073 Å, graphite monochromator). With an exposure time of 10 s, a frame width of 2°, and a detector distance of 50 mm, a total of 568 frames were collected in four $\omega$ scans ($\omega$ = −41° to 63°; $\kappa$ = −79°; $\theta$ = 30°; $\varphi$ = 0°, 90°, 180°, and 270°) and two $\varphi$ scans ($\varphi$ = 0° to 360°; $\omega$ = 0°; $\kappa$ = 0°; $\theta$ = 30°, −30°). The Oxford CrysAlis RED software[35] was used for data processing, including an empirical absorption correction with ABSPACK. In both cases, XPREP[36] was used for space group assignment and data merging (identical indices only), and the programs XS[37,38] and XL[38,39] were used for structure solution (direct methods) and structure refinement (full-matrix least-squares on $F_o^2$), respectively. Selected crystallographic data and refinement details are given in Tables 1 and 2 and in the Supporting Information, Table S-1 (anisotropic displacement parameters). Atomic coordinates were standardized with the program STRUCTURE TIDY[40] implemented in PLATON.[41]

**Table 1. Selected Crystallographic, Data Collection, and Refinement Data for $Li_3Zn_2Sn_4$ and $Li_2ZnGe_3$**

| | | |
|---|---|---|
| formula | $Li_3Zn_2Sn_4$ | $Li_2ZnGe_3$ |
| fw, $M$ ($g \cdot mol^{-1}$) | 626.32 | 297.02 |
| space group | $P6_3/mmc$ (No. 194) | $P6_3/mmc$ (No. 194) |
| $Z$ | 2 | 1 |
| unit cell parameters | | |
| $a$ (Å) | 4.528(1) | 4.167(1) |
| $c$ (Å) | 22.119(2) | 6.754(1) |
| $V$ (Å$^3$) | 392.78(4) | 101.58(3) |
| $\rho_{calc}$ ($g \cdot cm^{-3}$) | 5.296 | 4.855 |
| abs coeff (Mo K$\alpha$), $\mu$ ($mm^{-1}$) | 18.42 | 27.57 |
| $F$(000) | 538 | 132 |
| cryst color, shape | dark silver lustrous, block | dark silver lustrous, block |
| $T$ (K) | 293 | 125 |
| $\lambda$(Mo K$\alpha$) (Å) | 0.71073 | 0.71073 |
| diffractometer | STOE IPDS 2T (imaging plate) | OXFORD Xcalibur3 (Sapphire 3 CCD detector) |
| Θ range | 5.20−27.09° | 5.65−30.95° |
| limiting indices | $-5 \le h \le 5$ | $-6 \le h \le 6$ |
| | $-5 \le k \le 5$ | $-3 \le k \le 6$ |
| | $-28 \le l \le 28$ | $-9 \le l \le 9$ |
| reflns/unique | 2970/208 | 973/81 |
| $R_\sigma$, $R_{int}$ | 0.008, 0.029 | 0.015, 0.036 |
| data/restraints/params | 208/0/16 | 81/1/8 |
| extinction coeff | 0.0044(5) | 0.084(8) |
| largest diff peak and hole (e Å$^{-3}$) | +0.915 and −0.645 | +0.816 and −0.609 |
| GOF on $F^2$ | 1.580 | 1.243 |
| $R_1$, $wR_2$ ($I > 2\sigma(I)$) | 0.023, 0.046 | 0.015, 0.033 |
| $R_1$, $wR_2$ (all data) | 0.024, 0.047 | 0.018, 0.033 |

$Li_3Zn_2Sn_4$ crystallizes in space group $P6_3/mmc$ (No. 194), with lattice parameters $a$ = 4.528(1) Å and $c$ = 22.119(2) Å. After initial refinement cycles including only the Sn1 (4f), Sn2 (4e), and Zn1 (4f) sites, the two Li sites Li1 (2c) and Li2 (4f) were obtained from the


dx.doi.org/10.1021/ic3011037 | Inorg. Chem. 2013, 52, 2809−2816

**Table 2. Atomic Coordinates and Equivalent Isotropic Displacement Parameters for $Li_3Zn_2Sn_4$ and $Li_2ZnGe_3$**

| atom | Wyck. | $x$ | $y$ | $z$ | $U_{eq}$[b] (Å$^2$) |
|---|---|---|---|---|---|
| | | | $Li_3Zn_2Sn_4$ | | |
| Sn1 | 4*f* | 1/3 | 2/3 | 0.5290(1) | 0.015(1) |
| Sn2 | 4*e* | 0 | 0 | 0.1835(1) | 0.013(1) |
| Zn1 | 4*f* | 1/3 | 2/3 | 0.6550(1) | 0.017(1) |
| Li2 | 4*f* | 1/3 | 2/3 | 0.1079(8) | 0.034(5) |
| Li1 | 2*c* | 1/3 | 2/3 | 1/4 | 0.016(5) |
| | | | $Li_2ZnGe_3$ | | |
| Ge/Zn1[a] | 4*f* | 1/3 | 2/3 | 0.0569(1) | 0.009(1) |
| Li1 | 2*b* | 0 | 0 | 1/4 | 0.026(3) |

[a]Ratio Ge/Zn fixed to 0.75:0.25 in refinement (see Experimental Section). [b]$U_{eq}$ is defined as one third of the trace of the orthogonalized $U_{ij}$ tensor.

difference Fourier map. Anisotropic displacement parameters for all Sn, Zn, and Li sites were used in the refinement. Refinement cycles with a free variable for the occupancy parameter of the Sn1, Sn2, and Zn2 sites showed that the Sn and Zn sites are all fully occupied. The occupancy parameters for Li sites can usually not be determined reliably from X-ray diffraction data if strong scattering atoms are present beside Li. For the Li−Zn−Sn title phase, refinement of the site occupancy factors for Li1 and Li2 lead to values of 0.88(12) and 1.01(11), respectively. Since full occupancy is within the (high) standard deviation for both Li1 and Li2, the final refinement was carried out assuming full occupancy of all sites. The final residual map (highest difference peak and hole of +0.915 e Å$^{-3}$ and −0.645 e Å$^{-3}$) gives no indication of an additional Li site. Including a third Li site (4e) corresponding to that reported for $Li_2Ga_2Sn$[42] (4f site there) was tested but rejected for the Li−Zn−Sn title phase. Disregarding this Li site and the full ordering of Zn and Sn in contrast to the Ga/Sn mixed occupancy, $Li_3Zn_2Sn_4$ (= $Li_{1.5}ZnSn_2$) and $Li_2Ga_2Sn$ can be regarded as isotypic.

The structure of $Li_2ZnGe_3$ is also described in space group $P6_3/mmc$ (No. 194), with lattice parameters $a$ = 4.167(1) Å and $c$ = 6.754(1) Å. The phase shows a stuffed hexagonal diamond (2H polytype) like structure. From the single-crystal X-ray diffraction data, no indication of a (partial) ordering of Zn and Ge could be deduced, and the phase is thus described as adopting a $CaIn_2$ type structure with only one Ge/Zn mixed occupied network site. Refinements of a LiGaGe type structure model, space group $P6_3mc$ (No. 186), with two sites for the network atoms were tested but did not lead to a description with a partial ordering of Zn and Ge. Free refinement of the occupancy parameter for the Li site led to a value of 1.01(9), and thus the Li site was treated as fully occupied in the final refinement. The Ge/Zn ratio for the occupancy of the network site was fixed to Ge/Zn = 0.75:0.25, since the composition $Li_2ZnGe_3$ qualifies as a Zintl compound and the phase was successfully synthesized from corresponding stoichiometric amounts of the elements (see above). Furthermore, this agrees with previous information about a hexagonal Ge-rich Li−Zn−Ge phase with a stuffed 2H diamond like structure:[14] The hexagonal lattice parameters $a$ = 4.173 Å and $c$ = 6.768 Å were reported; it was noted that the structure is closely related to that of LiGaGe[43] but with (partial) Ge/Zn mixed occupancy, and the phase was referred to as "$Li_{1.14}Zn_{0.48}Ge_{1.37}$" (Ge/Zn ≈ 3:1) since (in the extensive phase analytical study on the Li−Zn−Ge system) it was obtained accompanied by the least amount of impurities (only traces of $\alpha$-Ge according to powder XRD analysis) from a reaction of the elements in that ratio.[14] However, a full structure determination has not yet been published for this phase; thus, the structure data for $Li_2ZnGe_3$, including atomic coordinates and displacement parameters, are reported here.

**EDX Measurements.** EDX analyses of single crystals of $Li_3Zn_2Sn_4$ and $Li_2ZnGe_3$ (unit cell determined by single-crystal XRD previous to EDX analysis) were carried out using a JEOL 5900LV scanning electron microscope equipped with an OXFORD INSTRUMENTS INCA energy-dispersive X-ray microanalysis system. The qualitative analysis showed the presence of Zn and Sn in case of $Li_3Zn_2Sn_4$ and Zn and Ge in case of $Li_2ZnGe_3$ and the absence of other elements heavier than Na.

**Electronic Structure Calculations.** DFT electronic structure calculations for $Li_3Zn_2Sn_4$ were carried out with the Stuttgart TB-LMTO-ASA program,[44] employing the tight-binding (TB) version of the linear muffin-tin orbital (LMTO) method in the atomic sphere approximation (ASA). The Barth−Hedin local exchange correlation potential[45] was used. Radii of the atomic spheres and interstitial empty spheres were determined by the procedures implemented in the TB-LMTO-ASA programs. The $k$-space integration was performed by the tetrahedron method.[46] Two sets of calculations were carried out: one using Li 2s/(2p)/(3d) states (downfolded in parentheses) as automatically selected by TB-LMTO-ASA program, and the other one not including 3d states for Li but only Li 2s/(2p). In both cases, Zn 4s/4p/3d and Sn 5s/5p/(5d)/(4f) states were included in the calculations (downfolded in parentheses), as automatically selected by the TB-LMTO-ASA program; 305 irreducible $k$-points were used. VESTA[47] was employed to prepare graphical representations of the ELF.

## RESULTS AND DISCUSSION

**Description of the Crystal Structures.** Both $Li_3Zn_2Sn_4$ and $Li_2ZnGe_3$ feature Li-stuffed diamond polytype like Zn−Tt (Tt = tetrel element) network substructures of four-connected atoms. The Zn−Sn substructure of $Li_3Zn_2Sn_4$ (Figures 1 and 2)

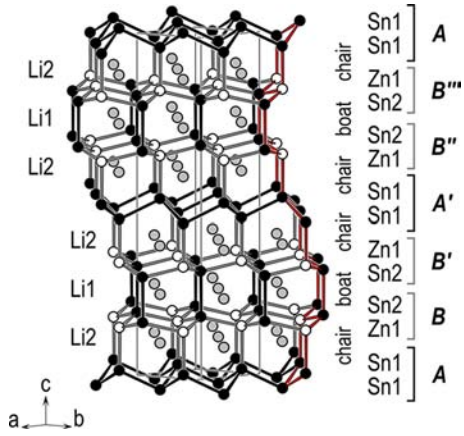


**Figure 1.** Crystal structure of $Li_3Zn_2Sn_4$. Li-stuffed 6H diamond polytype like Zn−Sn network. Li, Zn, and Sn atoms are represented with gray, white, and black spheres, respectively.

represents a 6H diamond polytype like structure with Zn and Sn atoms fully ordered on three sites (Sn1, Sn2, Zn1). In the case of $Li_2ZnGe_3$ (Figures 3 and 4), the Zn−Ge substructure is a 2H diamond polytype like network structure, and no indication for an ordering of Zn and Ge atoms on different networks sites was deduced from the X-ray diffraction data.

The 6H diamond polytype like Zn−Sn network of $Li_3Zn_2Sn_4$ is composed of two types of puckered layers of six-membered rings. Layer type A is exclusively built of Sn atoms (Sn1 on 4f) and the intralayer Sn1−Sn1 distance is 2.912(1) Å. Layer type B shows alternating Sn and Zn atoms (Sn2 on 4e, Zn1 on 4f) with a Sn2−Zn1 distance of 2.690(1) Å and is less puckered than layer type A. The layers extend parallel $ab$, and they are stacked along $c$ in the sequence ABB′A′B″B‴ (Figure 1). A- and B-type layers are connected via Sn1−Zn1 heteronuclear bonds (2.786(1) Å) and six-membered rings in chair conformation occur between them. Neighboring B-type layers are linked via homonuclear Sn2−Sn2 bonds (2.941(1) Å) that


dx.doi.org/10.1021/ic3011037 | Inorg. Chem. 2013, 52, 2809−2816

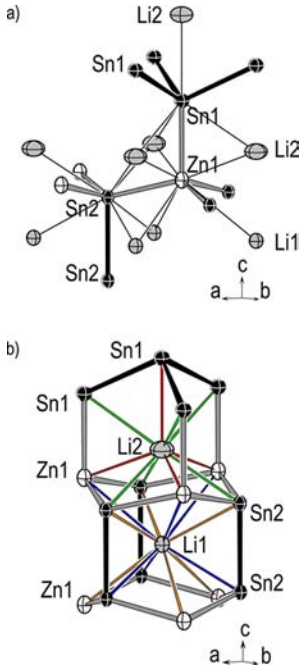


**Figure 2.** Coordination environments in the structure of $Li_3Zn_2Sn_4$. (a) Coordination of Zn and Sn atoms. (b) Coordination of the Li atoms. Thermal ellipsoids with 70% probability level. Li, Zn, and Sn atoms are represented with gray, white, and black ellipsoids, respectively. Zn−Sn contacts are represented with thick gray lines, Sn−Sn contacts with thick black lines, Li−Zn and Li−Sn contacts in panel a with thin black lines and in panel b with thin colored lines. Red and green lines represent the location in tetrahedral and octahedral voids, respectively, of the arrangements forming the 3C diamond polytype like part of the network, blue and orange lines represent the location in the octahedral voids in the 2H like part (see Discussion).

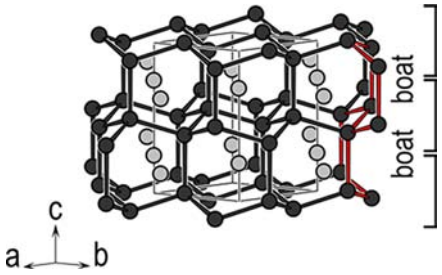


**Figure 3.** Crystal structure of $Li_2ZnGe_3$. Li-stuffed 2H diamond polytype like Zn−Ge network. Li atoms and atoms on the Ge/Zn sites are represented with light and dark gray spheres, respectively.

are part of interlayer six-membered rings in boat conformation. Note that occupation of the Zn1 site does not lead to the formation of Zn−Zn bonds. The Li atoms (Li1 on 2c, Li2 on 4f) are located in the voids of the Zn−Sn substructure (Figure 1), with Li−Zn and Li−Sn distances in the range from 2.814(6) to 3.355(1) Å. The coordination environments in $Li_3Zn_2Sn_4$ are shown in Figure 2; interatomic distances are listed in Table 3.

The Sn−Sn distances in $Li_3Zn_2Sn_4$ (2.912(1) and 2.941(1) Å) are slightly longer than the covalent bond distance in $\alpha$-Sn (2.810 Å). They are in the range of distances found for covalently bonded Sn polyanions such as in the Zintl phase $NaSn_2$[48] (2.822(1)−2.975(2) Å) or the covalent substructure in $NaSn_5$[49] (2.794(1)−2.886(1) Å). The Zn−Sn distances (2.690(1) and 2.786(1) Å) are also slightly longer than the sum of covalent radii (2.61 Å; according to ref 50) and match the

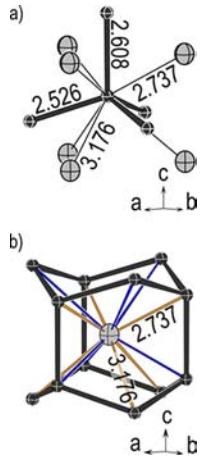


**Figure 4.** Coordination environments in the structure of $Li_2ZnGe_3$. (a) Coordination of Ge or Zn atoms on the Ge/Zn site. (b) Coordination of the Li atoms. Thermal ellipsoids with 70% probability level. Li atoms and atoms on the Ge/Zn site are represented with light and dark gray ellipsoids, respectively. Ge/Zn−Ge/Zn contacts are represented with thick dark gray lines, Li−Ge/Zn contacts in panel a with thin black lines, and those in panel b with thin colored lines. The coloring (blue and orange) indicates the location in the octahedral voids in the 2H like network (see Figure 2).

**Table 3. Interatomic Distances and −ICOHP (at $E_F$) Values for $Li_3Zn_2Sn_4$**

| atoms | | mult. | distance (Å) | −ICOHP (at $E_F$) (eV/bond) calculation with Li 2s/(2p) | −ICOHP (at $E_F$) (eV/bond) calculation with Li 2s/(2p)/(3d) |
|---|---|---|---|---|---|
| Sn1 | −Sn1 | 3× | 2.912(1) | 1.85 | 2.01 |
| | −Zn1 | 1× | 2.786(1) | 1.51 | 1.62 |
| | −Li2 | 1× | 3.029(2) | 0.32 | 0.31 |
| | −Li2 | 3× | 3.14(1) | 0.27 | 0.26 |
| Sn2 | −Zn1 | 3× | 2.690(1) | 1.89 | 2.01 |
| | −Sn2 | 1× | 2.941(1) | 1.73 | 1.85 |
| | −Li1 | 3× | 3.000(1) | 0.30 | 0.29 |
| | −Li2 | 3× | 3.103(9) | 0.24 | 0.25 |
| Zn1 | −Li1 | 3× | 3.355(1) | 0.09 | 0.09 |
| | −Li2 | 3× | 2.814(6) | 0.21 | 0.21 |
| Li1 | −Li2 | 1× | 3.14(2) | 0.03 | 0.03 |

Zn−Sn distances in the network of four-connected Zn and Sn atoms in $Na_5Zn_{2.28}Sn_{9.72}$ (2.717(1)−2.840(1) Å)[8] and the interatomic distance for cubic $Li_2ZnSn$ (2.792 Å).[21]

In the structure model for $Li_2ZnGe_3$ there is only one mixed occupied Ge/Zn site (4f) for the atoms in the 2H diamond polytype like network structure (Figure 3). The interatomic distance within the puckered layers of six-membered rings is 2.526(1) Å, and the interlayer bond length is 2.608(1) Å. The Li site (2b) is located between the layers (Figure 3), the Li−Ge/Zn distances are 2.737(1) and 3.176(1) Å. Figure 4 displays the coordination environments in $Li_2ZnGe_3$ and also gives the interatomic distances.

The interatomic distances in the Zn−Ge network of $Li_2ZnGe_3$ (2.526(1) and 2.608(1) Å) lie between the distance in $\alpha$-Ge (2.445 Å) or the sum of covalent radii for Zn and Ge (2.42 Å; according to ref 50) and the interatomic distance in cubic $\alpha$-$Li_2ZnGe$ (2.647 Å; single crystal data 173 K).[13]

**Discussion.** $Li_3Zn_2Sn_4$ and $Li_2ZnGe_3$ represent stuffed diamond polytype like structures, with Li atoms occupying the voids of the network that is formed by the Zn and Tt atoms.


dx.doi.org/10.1021/ic3011037 | Inorg. Chem. 2013, 52, 2809−2816

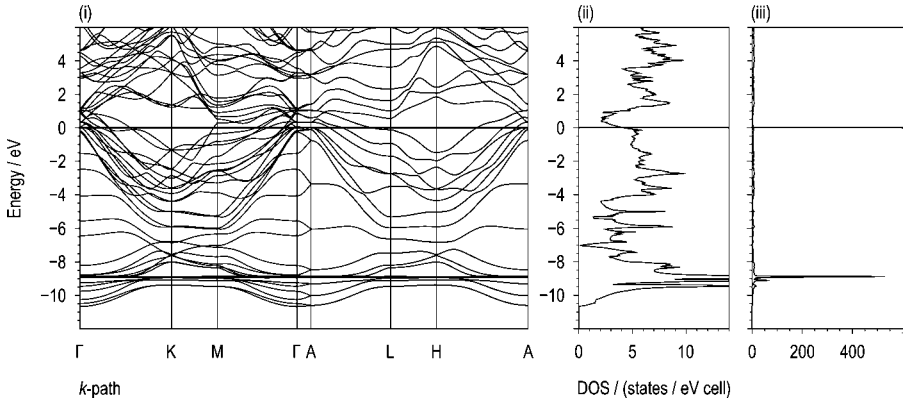


**Figure 5.** Band structure plot (i) and total DOS curves (ii, iii) for $Li_3Zn_2Sn_4$. TB-LMTO-ASA calculation with Li 2s and downfolded Li 2p. Fermi level ($E_F$) at 0 eV. The results of the calculation including downfolded Li 3d in the basis set are shown in the Supporting Information, Figure S-1.

Both phases show the same overall ratio of guest atoms (G) to atoms that build the host network (N), namely G/N = 1:2 ($Li_3Zn_2Sn_4$ = $Li(Zn_{0.33}Sn_{0.67})_2$; $Li_2ZnGe_3$ = $Li(Zn_{0.25}Ge_{0.75})_2$). Notably, the composition $Li_2ZnGe_3$ qualifies as an electron-precise Zintl phase, while $Li_3Zn_2Sn_4$ is one electron per formula unit short to be a valence compound. Stuffed diamond polytype like structures have been reported for a number of ternary Li−Tr−Tt (Tr = group 13 element) and Li−T−Tt phases (T = late d block element). Ratios of Li/Tr = 1:1 or with T = Zn, for example, Li/Zn = 2:1 relate to electron-precise Zintl phases according to a description with $Li^+$ cations and a polyanionic network of formally iso(valence)electronic $(4b\text{-}Tr)^-$ or $(4b\text{-}Zn)^{2-}$, respectively, and $(4b\text{-}Tt)^0$ atoms (4b = four-bonded).

The cubic 3C and the hexagonal 2H diamond structure can be described as cubic and hexagonal close packed (ccp and hcp), respectively, arrangement of N atoms with one-half of the tetrahedral voids occupied by the same type atoms N. Correspondingly, with two types of network atoms, N1 and N2, an ordered zinc blende and wurtzite like network structure (N1/N2 = 1:1) may be viewed as ccp and hcp, respectively, type array of N1 atoms with one-half of the tetrahedral void sites occupied by N2 atoms, or vice versa.

In 3C like structures, both the remaining tetrahedral and the octahedral voids can be filled by guest atoms. In 2H like structures generally only the octahedral void sites can be occupied, since filling the remaining tetrahedral voids would lead to filled face sharing tetrahedra, which is unfavorable due to the associated short interatomic distances. If one type of void is fully occupied, the resulting composition is $GN_2$ (with N = N1 + N2 + ...). If all remaining voids are filled, the composition is GN. Examples are the cubic Zintl phases LiAlGe[51−54] ($GN_2$) and $\alpha$-$Li_2ZnGe$[13] (GN) and hexagonal LiGaGe ($GN_2$) type structures.[55]

Besides such examples with ordered zinc blende or wurtzite like networks and fully occupied voids, there are also ternary phases with statistically occupied N1/N2 network sites, different N1/N2 ratios (statistical occupancy or ordered superstructure), or partially occupied voids. As an example, $Li_2AuSn_2$[56] (with a $G_2N_3$ composition) shows an ordered 3C like Au−Sn network (3-fold superstructure with respect to a cubic diamond structure) and a (fully occupied) Li site that leads to the occupancy of 2/3 of each of the tetrahedral and octahedral voids of a ccp array. Also mixed occupancy with Li on network sites or N on void sites has been reported for a number of phases.[9] The disorder is often related to a homogeneity range.[9] Besides, if N1 and N2 have almost the same atomic number like Zn and Ge, it is usually not possible to distinguish between statistical occupancy and an ordered structure on the basis of single-crystal X-ray diffraction data. Also the Li sites (and even more the site occupancy factors) are often difficult to determine in structures with strongly scattering N atoms.

Most stuffed diamond like structures of ternary phases with Tt elements feature 3C like networks, while examples with 2H like and other diamond polytype like structures are rather rare. The title phase $Li_3Zn_2Sn_4$ represents an example with a 6H polytype like network structure, similar to $Li_2Ga_2Sn$.[42] In the case of $Li_3Zn_2Sn_4$, Zn and Sn are fully ordered on the three network sites, in contrast to the Ga/Sn mixed occupancy described for $Li_2Ga_2Sn$ (Ga/Sn = 0.67:0.33 for all three sites).[42] The 6H polytype structure can be viewed as an intergrowth structure of a cubic and a hexagonal diamond like part in ratio 2:1 (see Figure 1, chair/boat = 2:1). In the crystal structure of $Li_3Zn_2Sn_4$, Li1 occupies the octahedral voids of the hexagonal diamond like part, which shows a ratio Zn/Sn = 1:1 but is not wurtzite like since there are Sn2−Sn2 homonuclear bonds between the two heteroatomic B-type layers. Li2 resides in one type of void in the cubic diamond like part, quasi-tetrahedrally coordinated by Sn1 and Zn1, and quasi-octahedrally by Sn2 and Sn1 (indicated in Figure 2b with red and green lines, respectively). In the structure model reported for $Li_2Ga_2Sn$, the same types of voids are also fully occupied, but additionally, there is a 50% occupancy of the second type of voids in the cubic diamond like part, leading to the composition $Li_2Ga_2Sn$ (G/N = 1:1.5), which corresponds to a Zintl phase (Li/Tr = 1:1). Though no indication for such a (partial) occupancy of these voids was deduced from the single-crystal XRD data for $Li_3Zn_2Sn_4$, the Li content of the phase is afflicted with some uncertainty, and also the existence of a phase width might be considered (see below). It should be noted however, that for $Li_2Ga_2Sn$ the Li sites were not deduced from the difference Fourier map (single-crystal XRD data). To the best of our knowledge, LiGaGe and $Li_2ZnGe_3$ (with Ge and same period Tr = Ga or T = Zn network atoms) are the only structurally characterized Li−Tr−Tt or Li−T−Tt phases with a wurtzite or 2H like structure. The structure of $Li_2ZnGe_3$ is described herein as $CaIn_2$ type, with a hexagonal 2H diamond like network with only one Ge/Zn mixed occupied site and Li occupying the octahedral voids. In this case, there also remains some uncertainty concerning the Ge/Zn ratio, since this cannot be verified on the basis of the X-ray diffraction data.


dx.doi.org/10.1021/ic3011037 | Inorg. Chem. 2013, 52, 2809−2816

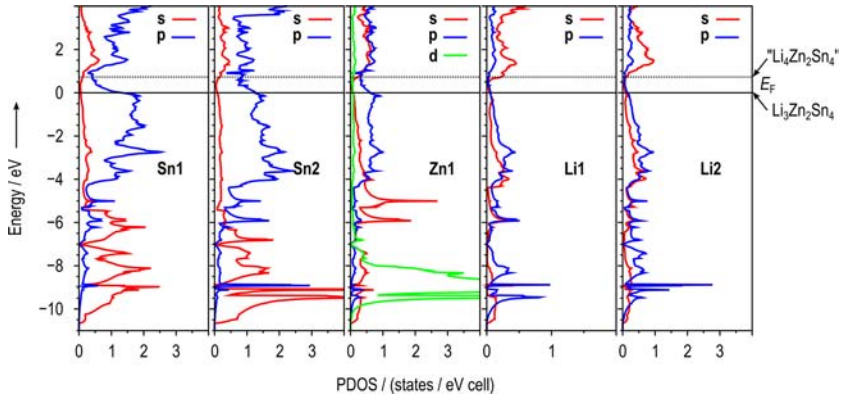


**Figure 6.** Partial density of states (PDOS) curves for $Li_3Zn_2Sn_4$. Fermi level ($E_F$) at 0 eV. The dotted line indicates the position of the IDOS (integrated DOS) value for a Zintl phase composition "$Li_4Zn_2Sn_4$" (within a rigid band model). TB-LMTO-ASA calculation with Li 2s and downfolded Li 2p. The results of the calculation including downfolded Li 3d in the basis set are shown in the Supporting Information, Figure S-2. Notice, different scales are used for the representation of the PDOS curves of atoms occupying Wyckoff sites with different multiplicity (Sn1, Zn1, and Li2 on 4f, Sn2 on 4e, Li1 on 2c).

$Li_3Zn_2Sn_4$ and $Li_2ZnGe_3$ are Tt-rich phases. As already discussed, $Li_2ZnTt$ phases with fully stuffed zinc blende like structures have been described for both Tt = Ge and Sn. So the Li−Zn−Tt (Tt = Ge, Sn) systems join the examples that show that phases with stuffed diamond polytype like structures can be found for quite different compositions in a ternary system.

**Electronic Structure Calculations.** The Stuttgart TB-LMTO-ASA programs[44] were used for DFT electronic structure calculations on $Li_3Zn_2Sn_4$. As described in the Experimental Section, two sets of calculations were carried out, differing in whether downfolded Li (3d) states were included.

The density of states (DOS) curves calculated without or with Li (3d) functions are very similar (see Figure 5 and Figure S-1 in the Supporting Information, respectively). The Fermi level ($E_F$ at 0 eV) is located at the edge of a pseudogap with a DOS minimum at approximately +0.5 eV. (It should be noted that bandgaps are generally underestimated by LDA-type calculations. Even for $\alpha$-Ge, for example, no bandgap at $E_F$ is found.) Notably, the IDOS (integrated DOS) value that, within a rigid band model, relates to a composition "$Li_4Zn_2Sn_4$" (= "$Li_2ZnSn_2$") can be found in the range of the pseudogap. ("$Li_2ZnSn_2$" would qualify as a charge-balanced Zintl phase with Li/Zn = 2:1). Also the analysis of the COHP (crystal orbital Hamilton population) plots (see Supporting Information) indicates that the bonding interactions would be optimized for a corresponding electron count. (That is, there are unoccupied bonding states above $E_F$ for $Li_3Zn_2Sn_4$.) So actually, a higher Li content seems favorable, and the results of the calculation for $Li_3Zn_2Sn_4$ thus suggest considering the existence of an electron-precise Zintl phase ("$Li_2ZnSn_2$") or a homogeneity range ("$Li_{3+x}Zn_2Sn_4$"). As discussed above, the crystal structure would allow accommodation of a higher Li content. However, the XRD single-crystal structure analysis led to the description of the phase as $Li_3Zn_2Sn_4$ since attempts to use a structure model with an additional Li site for the refinement failed (see Experimental Section).

PDOS (partial DOS) plots are shown in Figure 6 and Figure S-2, Suppporting Information (calculation without or with Li (3d) functions, respectively). As shown by the PDOS analyses for the Zn and Sn atoms, Zn-p and Sn-p states prevail at and close to the Fermi level. Zn acts as a "pseudo-main group metal", with the Zn-d states as "pseudo-core states" giving rise to the main DOS peak at approximately −9 eV (see iii of Figure 5 and Figure S-1, Suppporting Information).

The −ICOHP (integrated COHP) values (at $E_F$) are given in Table 3. Employing or not employing Li (3d) states leads to slightly different −ICOHP values, but the general trends are not affected by this choice. The highest −ICOHP (at $E_F$) values are found for the Sn1−Sn1 and Zn1−Sn2 bonds within the A- and B-type layers, respectively. The interlayer contacts, Sn2−Sn2 and Sn1−Zn1, are associated with slightly lower −ICOHP values, corresponding to the slightly longer interatomic distances. The −ICOHP values for the Li−Sn and Li−Zn contacts are low ($\leq$ 0.32). So the −ICOHP values reveal significant Sn−Sn and Zn−Sn bonding interactions, consistent with the description of $Li_3Zn_2Sn_4$ as a polar intermetallic phase with a polyanionic Zn−Sn network.

The covalent Sn−Sn bonds are also apparent from representations of the electron localization function (ELF). ELF representations obtained from the calculation with Li 2s/(2p) or Li 2s/(2p)/(3d) are depicted in Figure 7 and Figure 8, respectively. The appearance of the ELF basins associated with the Sn1−Sn1 bond (① in Figure 7a; ⑤ in Figure 8a) and the Sn2−Sn2 bond (② in Figure 7b; ⑥ in Figure 8b) is typical for covalent two-center bonds like those in $\alpha$-Sn. Further, it is essentially unaffected by the different choice of basis set for Li, as it can be seen from a comparison of Figures 7 and 8. This is different for the remaining valence basins of the Sn1 and Sn2 atoms. The ELF analysis for the calculation without Li (3d) leads to the situation shown in Figure 7: For Sn1, the reducible localization domain ③ (Figure 7a) comprises three maxima, each located *between* two of the Sn1−Li2 connecting lines. This could be interpreted in terms of multicenter bonding interactions. For intermediate ELF isovalues (e.g., ELF = 0.45 as shown in Figure 7a) ③ leaves a circular opening around the interlayer Sn1−Zn1 connecting line. The reducible localization domain ④ at Sn2 (Figure 7b) features lobes on the three Sn2−Zn1 bond vectors and further includes a maximum on the 3-fold axis of symmetry (parallel *c*). The ELF representations based on the calculation including Li (3d) states, depicted in Figure 8, show basins ⑦ (Figure 8a) or ⑧ (Figure 8b) on each of the three (symmetry equivalent) Sn1−Li2 or Sn2−Li2 connecting lines, respectively, suggesting directed Sn−Li interactions. Lone pair like basins of tetrel atoms that are oriented toward Li have been described in ELF analyses (based


dx.doi.org/10.1021/ic3011037 | *Inorg. Chem.* 2013, 52, 2809−2816

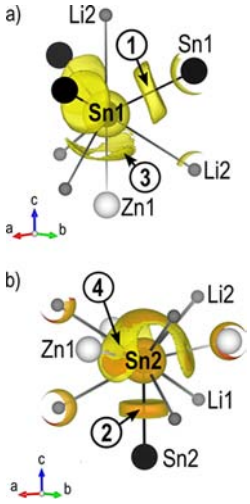


**Figure 7.** Isosurface representations of the ELF for $Li_3Zn_2Sn_4$. TB-LMTO-ASA calculation with Li 2s and downfolded Li 2p. (a) Valence basins ① and ③ of the Sn1 atoms of the A-type layer (see Figure 1). ELF isovalue 0.45. (b) Valence basin ② and merged valence basin ④ of the Sn2 atoms of the B-type layer. ELF isovalues 0.46 (yellow) and 0.475 (red).

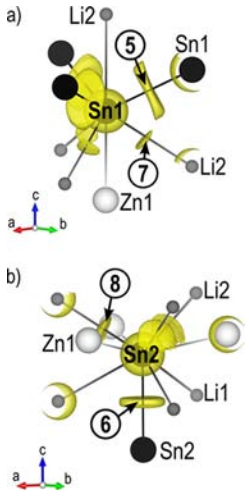


**Figure 8.** Isosurface representations of the ELF for $Li_3Zn_2Sn_4$. TB-LMTO-ASA calculation with Li 2s and downfolded Li 2p and Li 3d. (a) Valence basins ⑤ and ⑦ of the Sn1 atoms of the A-type layer (see Figure 1). ELF isovalue 0.50. (b) Valence basins ⑥ and ⑧ of the Sn2 atoms of the B-type layer. ELF isovalue 0.50.

on calculations with Li 2s/(2p)/(3d)) for other polar intermetallics or Zintl phases with Li and Tt elements, for example, in ref 57. Such directed Li−Sn interactions could be related to the high polarizing power of Li. Further note the diagonal relationship between Li and Mg and the discussion of covalent Mg−Sn bonds in intermetallic phases as in the recent account on $Na_2MgSn$.[58] In this context, it is also worth noting that for certain intermetallic Li−T−Sn or Mg−T−Sn phases also Li/Sn or Mg/Sn, respectively, mixed occupancy has been described, see for example refs 9, 59, and 60.

Leaving the question of which Li basis set should be preferred open to debate, the fact that the localization domains that might be associated with Zn−Sn or Li−Sn interactions are strongly influenced by the choice of basis set for Li suggests to view them as lone pair like basins of the Sn atoms, which are, in shape and alignment, adjusted to the surroundings. So, in contrast to the homonuclear Sn−Sn bonds, the heteronuclear Zn−Sn contacts in the network of four-bonded Zn and Sn atoms are not associated with ELF basins that can unambiguously be related to covalent two-center bonds. The ELF rather shows the differences between the Zn−Sn and the Sn−Sn bonding interactions within the Zn−Sn polyanionic network.

## CONCLUSION

The structural chemistry of alkali metal−zinc−germanides and stannides shows noticeable similarities to that of related ternary alkali metal−trielid−tetrelides. The late d block metal Zn can play a similar role as its direct neighbors from the p block, engaging in Zn−Tt polyanions, which are analogous to (pure main group) Tr−Tt polyanions. With the smallest alkali metal Li, diamond polytype like Zn−Tt networks are common polyanion structures, as exemplified by the title phases $Li_2ZnGe_3$ and $Li_3Zn_2Sn_4$. These represent rare examples of stuffed 2H and 6H, respectively, polytype like network structures, and $Li_3Zn_2Sn_4$ further stands out due to its ordered structure with no mixed occupancy on the network sites. In view of a possible variation of the Li content in the stuffed diamond like structure and its metallic behavior, which is indicated by the calculated band structure, $Li_3Zn_2Sn_4$ seems to bear interesting properties relevant for anode materials in battery research. Due to the pseudogap of $Li_3Zn_2Sn_4$ just above $E_F$ and possible multicenter bonding including contacts between framework and Li atoms, doping of the stannide could lead to an sp-bonded semiconducting network phase with a small band gap as shown by thermoelectric materials.[6]

## ASSOCIATED CONTENT

### Supporting Information

X-ray crystallographic files in CIF format for the title compounds, tables of anisotropic displacement parameters, band structure plot, total DOS, and PDOS curves for $Li_3Zn_2Sn_4$ from TB-LMTO-ASA calculation with Li 2s/(2p)/(3d), and −(I)COHP curves for $Li_3Zn_2Sn_4$ from TB-LMTO-ASA calculation with Li 2s/(2p) and from TB-LMTO-ASA calculation with Li 2s/(2p)/(3d). This material is available free of charge via the Internet at http://pubs.acs.org.

## AUTHOR INFORMATION

### Corresponding Author

*E-mail: Thomas.Faessler@lrz.tum.de.

### Notes

The authors declare no competing financial interest.

## ACKNOWLEDGMENTS

S.S. appreciates a Ph.D. fellowship from the *Studienstiftung des Deutschen Volkes*. This work was financially supported by Grant FA 198/11-1 of the *Deutsche Forschungsgemeinschaft* within the *Materials World Network* program. We thank V. Baran, A. Henze, and F. Krause who carried out supporting experimental work on the synthesis of the title phases.

## REFERENCES

(1) Graf, T.; Felser, C.; Parkin, S. S. P. *Prog. Solid State Chem.* **2011**, *39*, 1.

(2) Caillat, T.; Fleurial, J.-P.; Borshchevsky, A. *J. Phys. Chem. Solids* **1997**, *58*, 1119.

(3) Snyder, G. J.; Christensen, M.; Nishibori, E.; Caillat, T.; Iversen, B. B. *Nat. Mater.* **2004**, *3*, 458.

(4) Nylén, J.; Andersson, M.; Lidin, S.; Häussermann, U. *J. Am. Chem. Soc.* **2004**, *126*, 16306.
(5) Wu, Y.; Nylén, J.; Naseyowma, C.; Newman, N.; Garcia-Garcia, F. J.; Häussermann, U. *Chem. Mater.* **2008**, *21*, 151.
(6) Häussermann, U.; Mikhaylushkin, A. S. *Dalton Trans.* **2010**, *39*, 1036.
(7) Kim, S.-J. Ph.D. Thesis, Technische Universität München, Germany, 2007.
(8) Ponou, S.; Kim, S.-J.; Fässler, T. F. *J. Am. Chem. Soc.* **2009**, *131*, 10246.
(9) Pöttgen, R.; Dinges, T.; Eckert, H.; Sreeraj, P.; Wiemhöfer, H.-D. *Z. Phys. Chem* **2010**, *224*, 1475.
(10) *Handbook of Battery Materials*, 2nd ed.; Claus, D., Besenhard, J. O., Eds.; Wiley-VCH: Weinheim, Germany, 2011.
(11) Belin, C.; Sportouch, S.; Tillard-Charbonnel, M. *C. R. Acad. Sci. II* **1993**, *317*, 769.
(12) Sportouch, S.; Belin, C.; Tillard-Charbonnel, M.; Rovira, M. C.; Canadell, E. *New J. Chem.* **1995**, *19*, 243.
(13) Lacroix-Orio, L.; Tillard, M.; Belin, C. *Solid State Sci.* **2006**, *8*, 208.
(14) Schönemann, H.; Schuster, H.-U. *Rev. Chim. Miner.* **1976**, *13*, 32.
(15) Schönemann, H.; Schuster, H.-U. *Z. Anorg. Allg. Chem.* **1977**, *432*, 87.
(16) Schuster, H.-U. *Naturwissenschaften* **1966**, *53*, 361.
(17) Schuster, H.-U. *Z. Anorg. Allg. Chem.* **1969**, *370*, 149.
(18) Cullmann, H. -O.; Hinterkeuser, H.-W.; Schuster, H.-U. *Z. Naturforsch. B* **1981**, *36*, 917.
(19) Lacroix-Orio, L.; Tillard, M.; Belin, C. *J. Alloy. Compd.* **2008**, *465*, 47.
(20) Cullmann, H.-O.; Schuster, H.-U. *Z. Anorg. Allg. Chem.* **1983**, *506*, 133.
(21) Pobitschka, W.; Schuster, H.-U. *Z. Naturforsch. B* **1978**, *33*, 115.
(22) Cheviré, F.; DiSalvo, F. J. *Acta Crystallogr.* **2007**, *E63*, i62.
(23) Xie, Q. Ph.D. thesis, Eidgenössische Technische Hochschule, Zürich, Switzerland, 2004.
(24) Queneau, V.; Sevov, S. C. *J. Am. Chem. Soc.* **1997**, *119*, 8109.
(25) Nolas, G. S.; Cohn, J. L.; Dyck, J. S.; Uher, C.; Yang, J. *Phys. Rev. B* **2002**, *65*, No. 165201.
(26) Nolas, G. S.; Weakley, T. J. R.; Cohn, J. L. *Chem. Mater.* **1999**, *11*, 2470.
(27) Kim, S.-J.; Hoffmann, S. D.; Fässler, T. F. *Angew. Chem., Int. Ed.* **2007**, *46*, 3144.
(28) Kim, S.-J.; Fässler, T. F. *J. Solid State Chem.* **2009**, *182*, 778.
(29) Kim, S.-J.; Kraus, F.; Fässler, T. F. *J. Am. Chem. Soc.* **2009**, *131*, 1469.
(30) Menges, E.; Hopf, V.; Schäfer, H.; Weiss, A. *Z. Naturforsch. B* **1969**, *24*, 1351.
(31) *WinXPOW* (Version 2.08), STOE & Cie GmbH, Darmstadt, Germany, 2003.
(32) *X-AREA* (Version 1.26), STOE & Cie GmbH, Darmstadt, Germany, 2004.
(33) *X-RED32* (Version 1.26), STOE & Cie GmbH, Darmstadt, Germany, 2004.
(34) *X-SHAPE* (Version 2.05), STOE & Cie GmbH, Darmstadt, Germany, 2004.
(35) *CrysAlis RED* (Version 1.171.33.34d), Oxford Diffraction Ltd., Abindon, U.K., 2009.
(36) *XPREP* (Version 6.14), Bruker Nonius, Delft, the Netherlands, 2003.
(37) *XS - Crystal Structure Solution - SHELXTL* (Version 6.12), Bruker AXS, Madison, WI, 2001.
(38) Sheldrick, G. *Acta Crystallogr.* **2008**, *A64*, 112.
(39) *XL - Crystal Structure Refinement - SHELXTL* (Version 6.12), Bruker AXS, Madison, WI, 2001.
(40) Gelato, L. M.; Parthe, E. *J. Appl. Crystallogr.* **1987**, *20*, 139.
(41) Spek, A. L. *Acta Crystallogr.* **1990**, *A46* (Supplement), c34.
(42) Blase, W.; Cordier, G.; Kniep, R. *Z. Anorg. Allg. Chem.* **1993**, *619*, 1161.
(43) Bockelmann, W.; Schuster, H.-U. *Z. Anorg. Allg. Chem.* **1974**, *410*, 233.
(44) Jepsen, O.; Burkhardt, A.; Andersen, O. K. *The Stuttgart TB-LMTO-ASA Program (Version 4.7)*, Max-Planck-Institut für Festkörperforschung, Stuttgart, Germany, 1998.
(45) Barth, U. v.; Hedin, L. *J. Phys. C: Solid State Phys.* **1972**, *5*, 1629.
(46) Blöchel, P. E.; Jepsen, O.; Andersen, O. K. *Phys. Rev. B* **1994**, *49*, 16223.
(47) Momma, K.; Izumi, F. *J. Appl. Crystallogr.* **2008**, *41*, 653.
(48) Dubois, F.; Schreyer, M.; Fässler, T. F. *Inorg. Chem.* **2004**, *44*, 477.
(49) Fässler, T. F.; Kronseder, C. *Angew. Chem., Int. Ed.* **1998**, *37*, 1571; *Angew. Chem.* **1999**, *110*, 1641.
(50) Cordero, B.; Gómez, V.; Platero-Prats, A. E.; Revés, M.; Echeverría, J.; Cremades, E.; Barragán, F.; Alvarez, S. *Dalton Trans.* **2008**, 2832.
(51) Nowotny, H.; Holub, F. *Monatsh. Chem.* **1960**, *91*, 877.
(52) Bockelmann, W.; Schuster, H.-U. *Z. Anorg. Allg. Chem.* **1974**, *410*, 241.
(53) Schuster, H.-U.; Hinterkeuser, H.-W.; Schäfer, W.; Will, G. *Z. Naturforsch. B* **1976**, *31*, 1540.
(54) Tillard, M.; Belin, C.; Spina, L.; Jia, Y. Z. *Acta Crystallogr.* **2005**, *C61*, I51.
(55) Note that the hexagonal void sites of the N1 hcp and those of the N2 hcp coincide (cf. Figures 3b and 4b).
(56) Wu, Z.; Mosel, B. D.; Eckert, H.; Hoffmann, R.-D.; Pöttgen, R. *Chem.—Eur. J.* **2004**, *10*, 1558.
(57) Xie, Q.; Nesper, R. *Z. Anorg. Allg. Chem.* **2006**, *632*, 1743.
(58) Yamada, T.; Deringer, V. L.; Dronskowski, R.; Yamane, H. *Inorg. Chem.* **2012**, *51*, 4810.
(59) Schlüter, M.; Häussermann, U.; Heying, B.; Pöttgen, R. *J. Solid State Chem.* **2003**, *173*, 418.
(60) Schlüter, M.; Kunst, A.; Pöttgen, R. *Z. Anorg. Allg. Chem.* **2002**, *628*, 2641.